



Non-destructive and Non-contact Stress-Strain Characterization of Aerospace Alloys and Coatings using Laser Infrared Photo-Thermo-Mechanical Radiometry (PTMR)

Andreas Mandelis^{1,2} , Huiting Huan^{1,2} and Alexander Melnikov¹

¹ *Center for Advanced Diffusion-Wave and Photoacoustic Technologies (CADIPT), Department of Mechanical and Industrial Engineering, University of Toronto, Toronto, Ontario M5S 3G8, Canada*

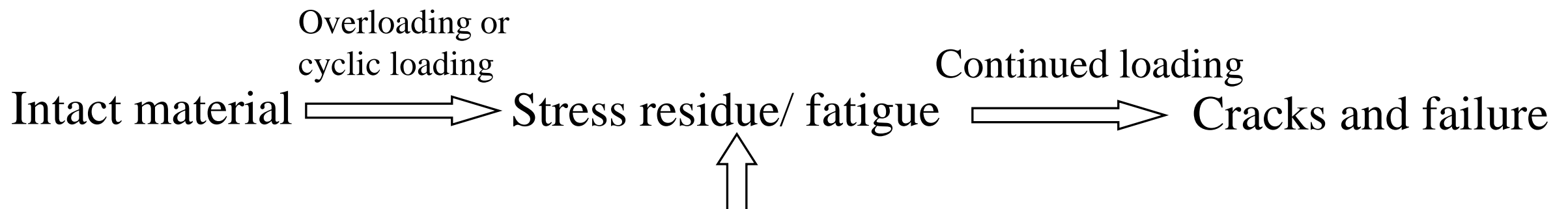
² *School of Optoelectronic Information, University of Electronic Science and Technology of China, Chengdu, Sichuan 610054, China*

- 1 Background: Mechanical strength evaluation for aerospace materials
- 2 Methodology: Laser Infrared Photo-Thermo-Mechanical Radiometry (PTMR)
- 3 Experiment: Non-contacting stress-strain relation characterized by the PTR signal
- 4 Theory and analysis: Quantification of experimental results through a 1-D thermo-mechanical-wave model
- 5 Results and Outlook: The present work gives rise to Photo-Thermo-Mechanical Radiometry (PTMR) as a non-destructive, non-contact strain gauge for the evaluation of mechanical strength of materials

Background



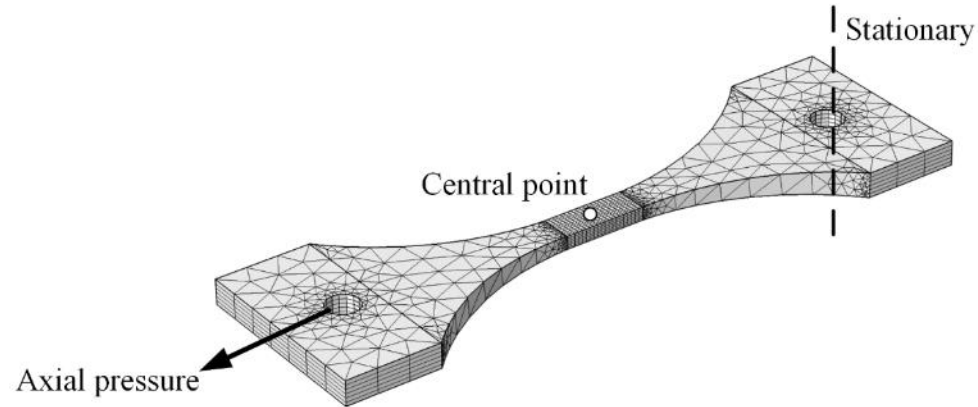
- Hidden fatigue underlies threat to safety in aerospace components



It will be of great value if the strength condition of the material can be evaluated before fatigue actually occurs!

Material Property

- Strength evaluation by FEM



- The sample is made of aluminum 6061-T6, a general material in aerospace industry
- Use linear elastic stress-strain constitutive equation and balance of force:

$$\boldsymbol{\tau} = \mathbf{C} : \boldsymbol{\varepsilon}$$

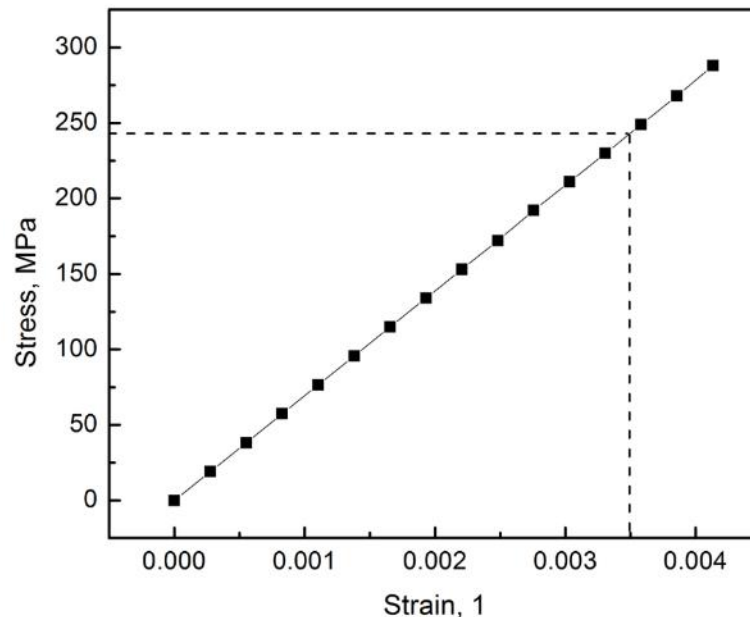
$$\nabla \cdot \boldsymbol{\tau} = -\mathbf{F}$$

$\boldsymbol{\tau}$ – stress tensor, $\boldsymbol{\varepsilon}$ – strain tensor, $\mathbf{C} = C_{ijkl}$ – modulus tensor of rank four ($i, j, k, l = 1, 2, 3, 4$), \mathbf{F} – external force.

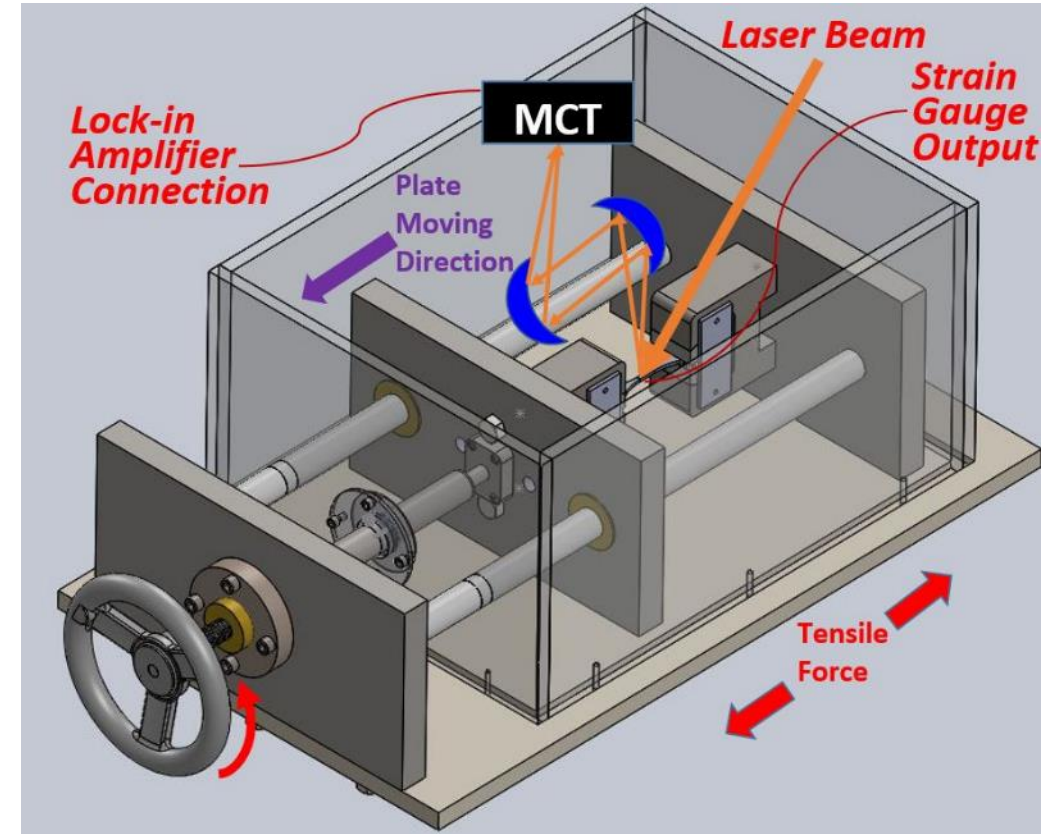
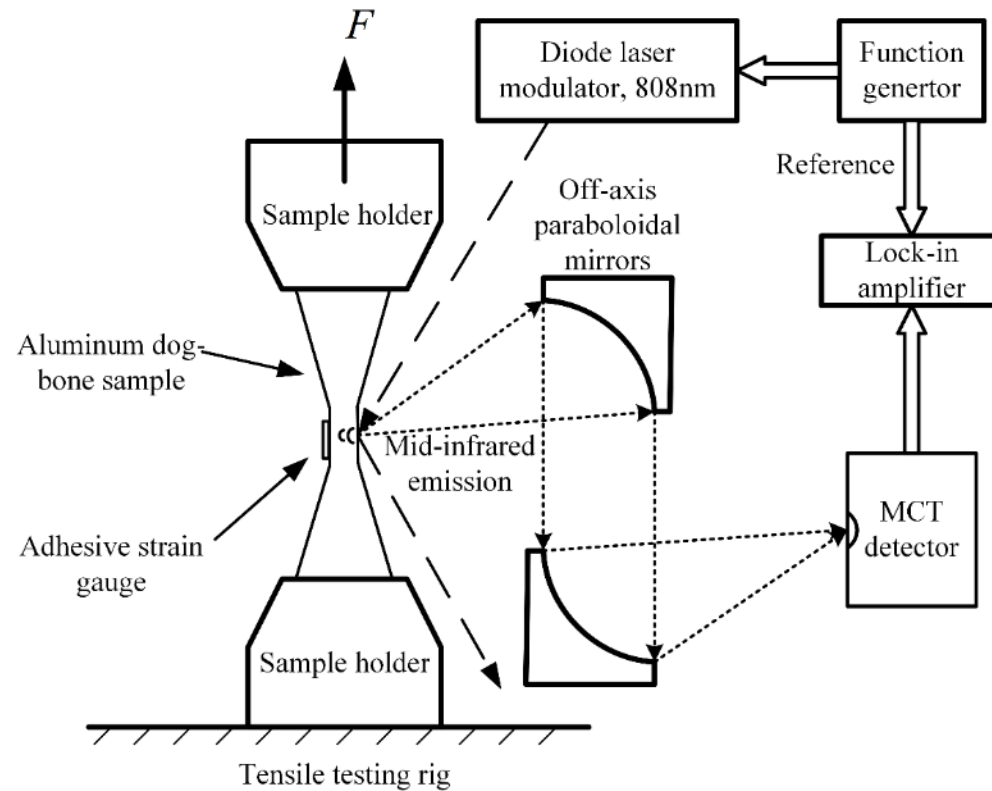
- According to ASTM 308, the elastic limit of this material is at least 240 MPa, which yields:

$$\varepsilon \leq 0.0035 (3500 \mu\text{m/m})$$

in terms of strain representation.



Methodology



Main advantages:

- Non-destructive when operated below the elastic ceiling.
- Totally non-contact and localized detection.

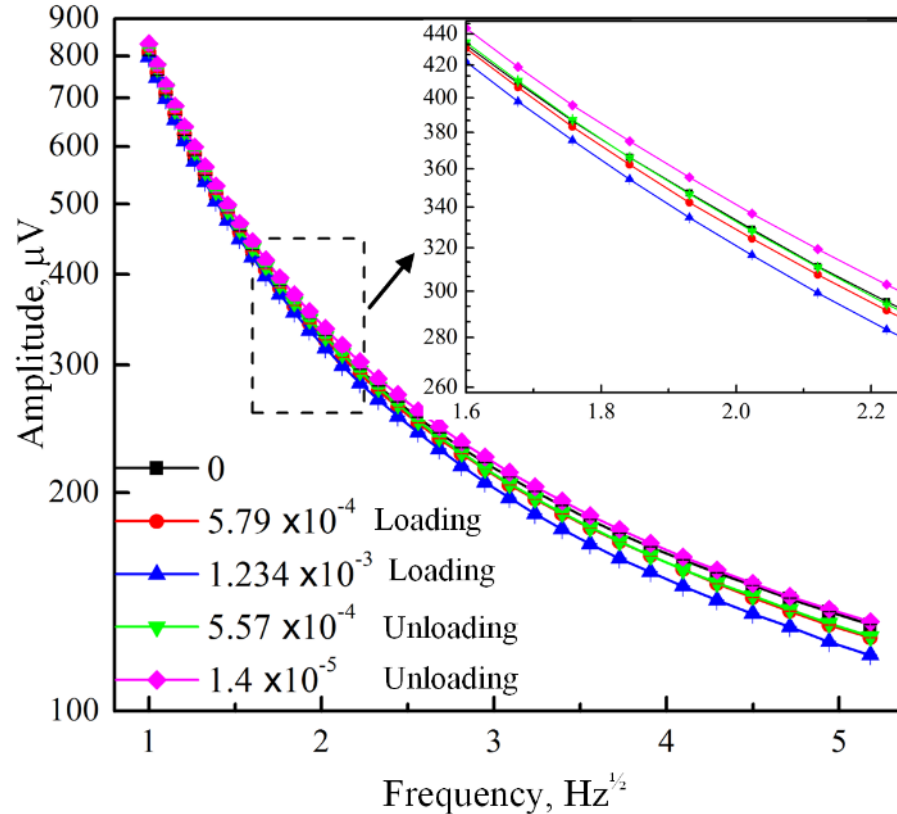
PTR signal: $S = A \exp[i(\omega t + \Phi)]$

Signal amplitude: $A = \|S\|$

Signal phase: $\Phi = \arg(S)$

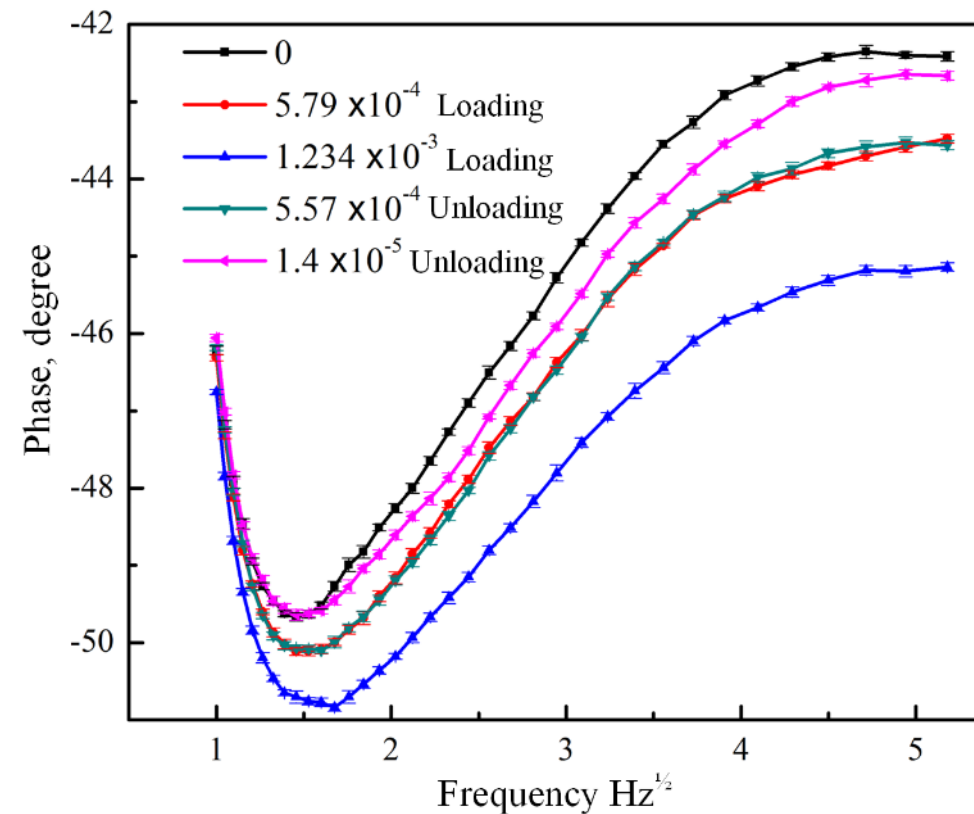
Experimental

Frequency-scan signal: 1-30 Hz (low frequency) $\mu(f) = \sqrt{\alpha / \pi f} \gg \Delta L$



(a)

Strain Unit: [1]



(b)

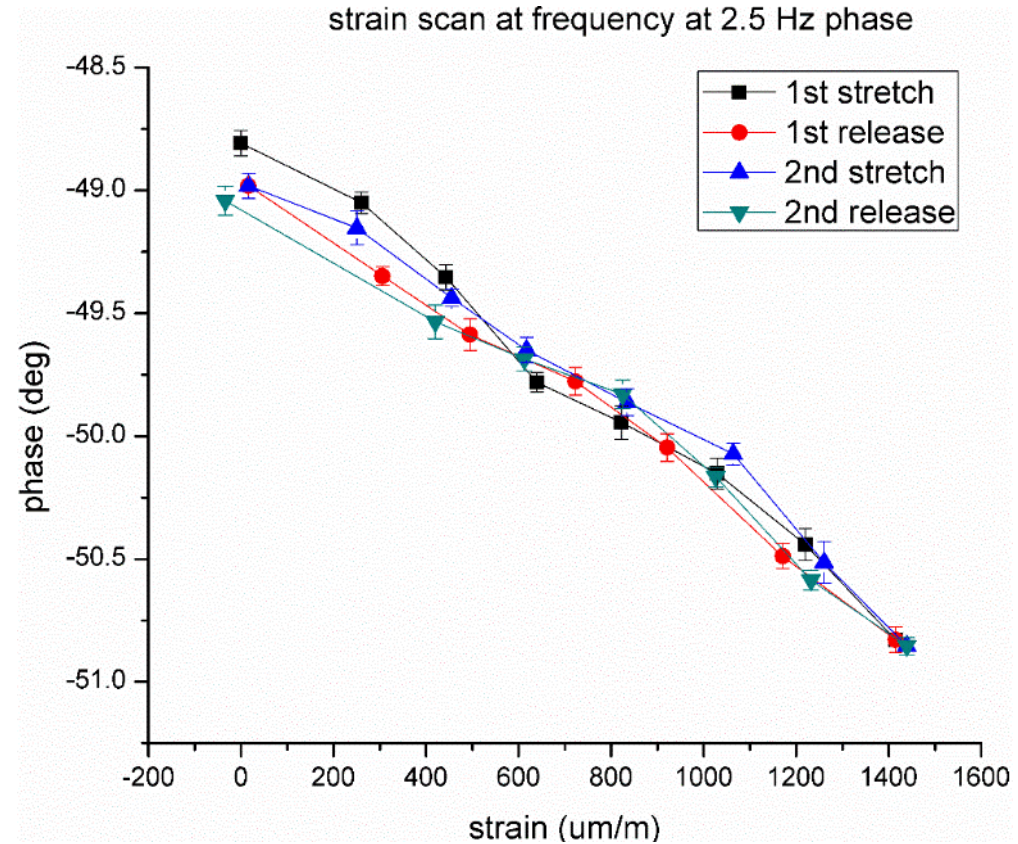
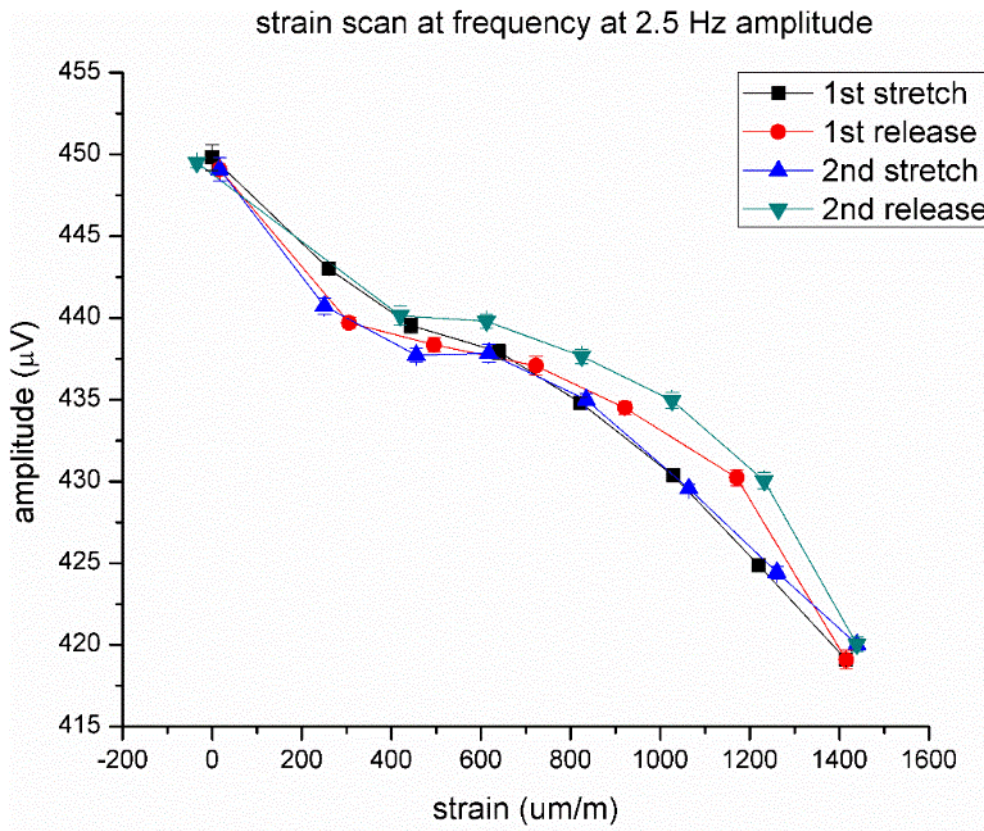
Stress condition: Within elastic regime.

Stress procedure: Loading and relaxing.

Good reproducibility and reversibility of the
PTR signal within the elastic regime!

Experimental Results

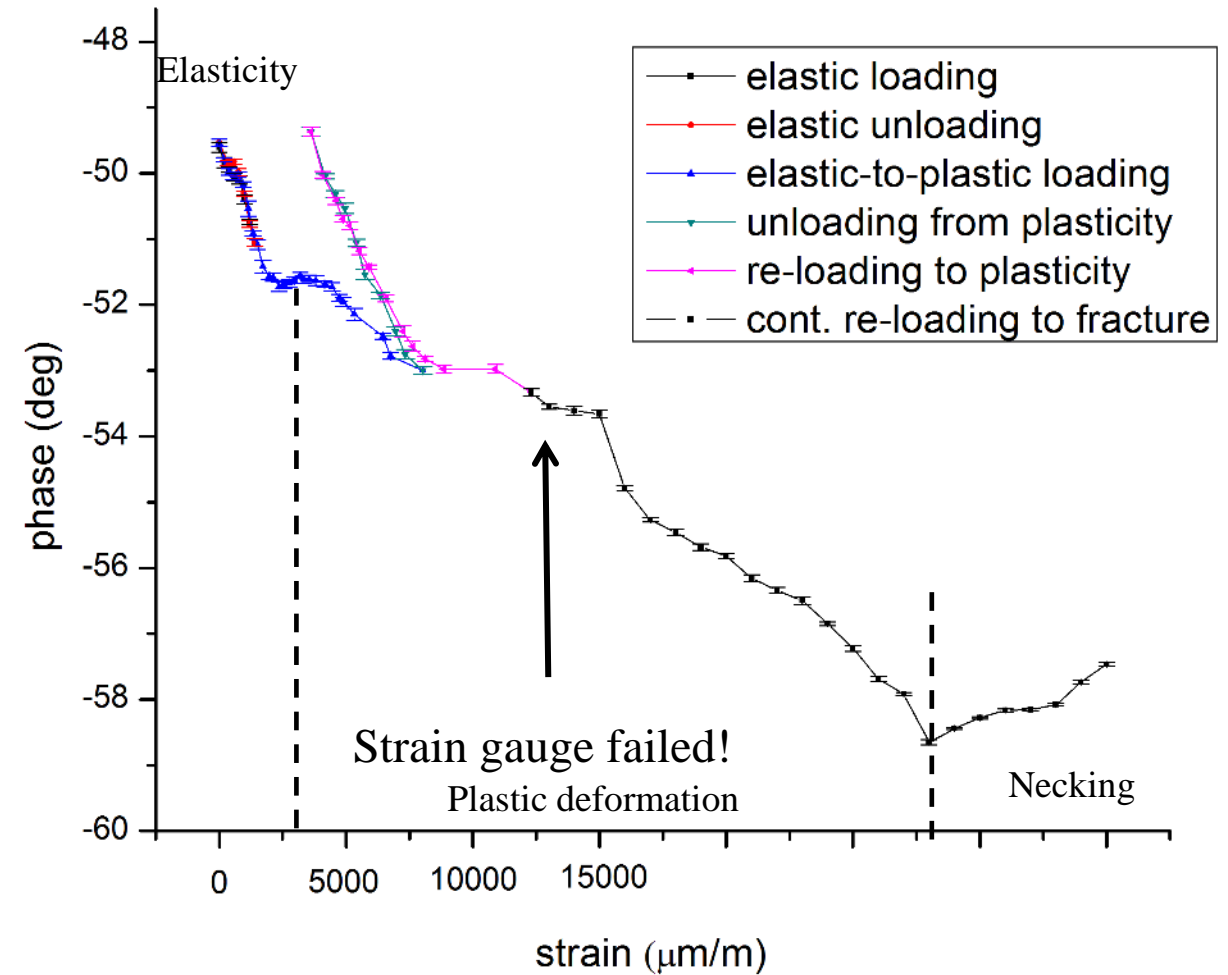
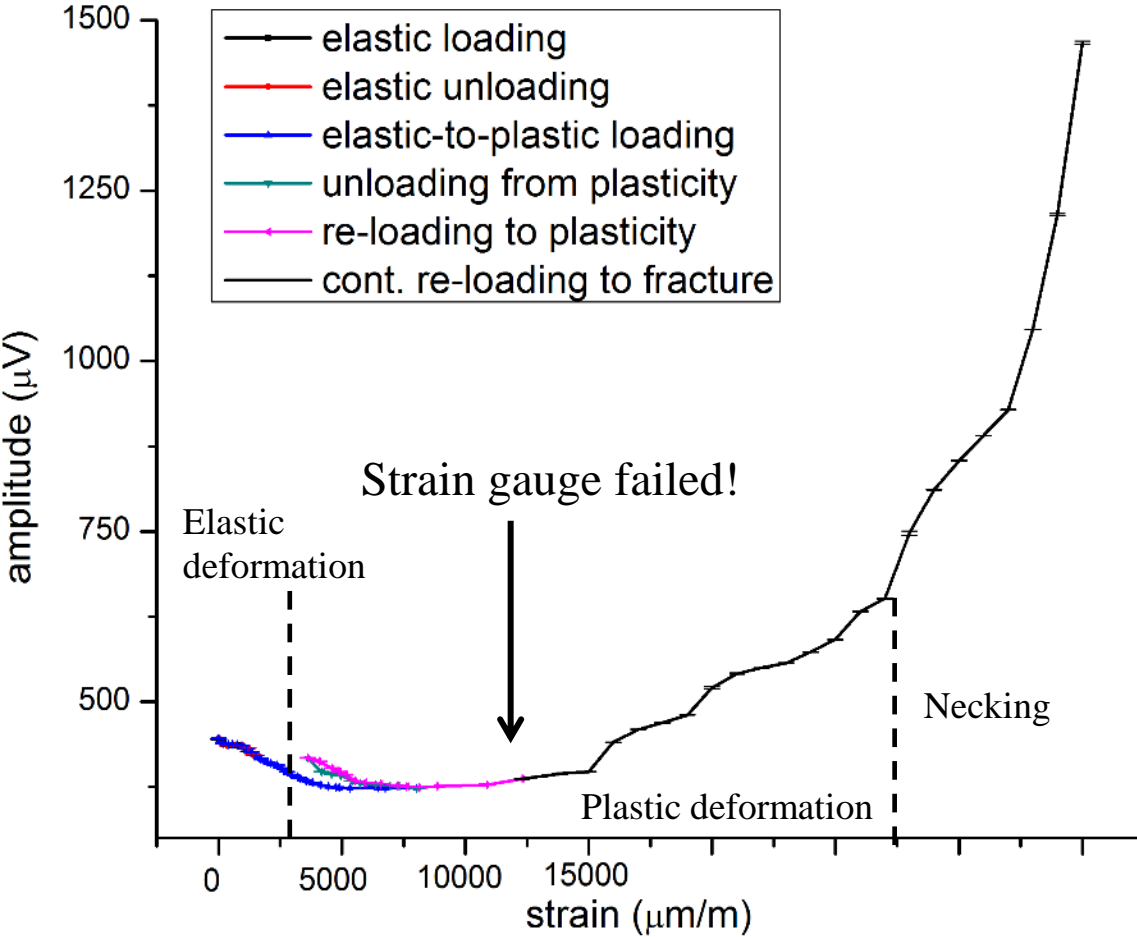
- Strain-scan result: stress free to $\sim 1400 \mu\text{m/m}$, within the elastic regime
- Set frequency at 2.5 Hz. Involving multiple loading and unloading process



The elastic loading and unloading test shows a good repeatable and reversible pattern. This indicates that the sample recovers its thermal properties after removal of tension within the elastic regime.

Experimental Results (cont'd)

- Signal strain dependence: beyond the elastic regime



- In the necking regime, the sample undergoes large deformation and thus the surface is deformed significantly, which drastically changes the PTR amplitude. Phase is less sensitive to this change and is more reliable as it is less affected by extraneous factors like surface curvature and shape change.

Theory and Analysis

- Frequency dependence of PTR signal

$$T(0, \omega) = \frac{\beta I(\omega)(1 + e^{-2\sigma_1 L})}{k_1 \sigma_1 (1 - e^{-2\sigma_1 L})} \quad (1)$$

$$\text{Amplitude: } A(\omega) \sim \|Y(\omega)\| I(\omega) \frac{1 + e^{-2\sigma_1 L}}{k_1 \sigma_1 (1 - e^{-2\sigma_1 L})} \quad (2)$$

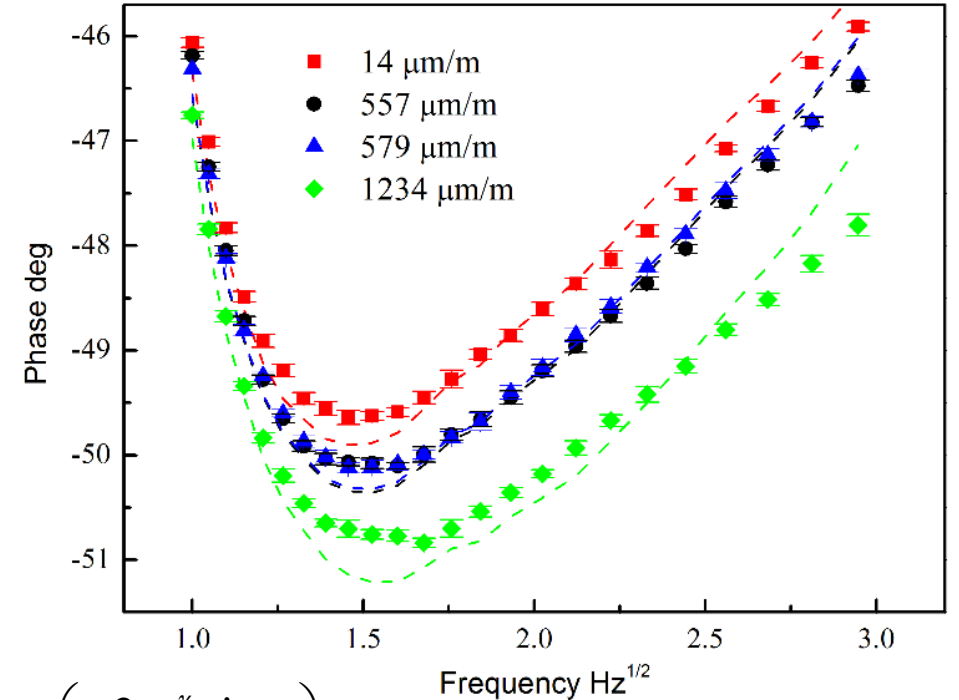
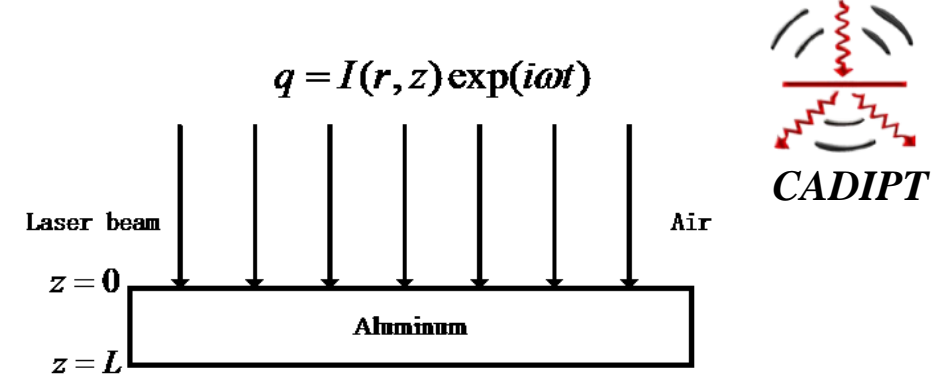
$$\text{Phase: } \Phi(\omega) = \arg\left(\frac{1 + e^{-2\sigma_1 L}}{1 - e^{-2\sigma_1 L}}\right) - \frac{\pi}{4} + \Phi_0(\omega) \quad (3)$$

$$\Phi_0(\omega) = \arg[Y(\omega)]$$

Normalized to:

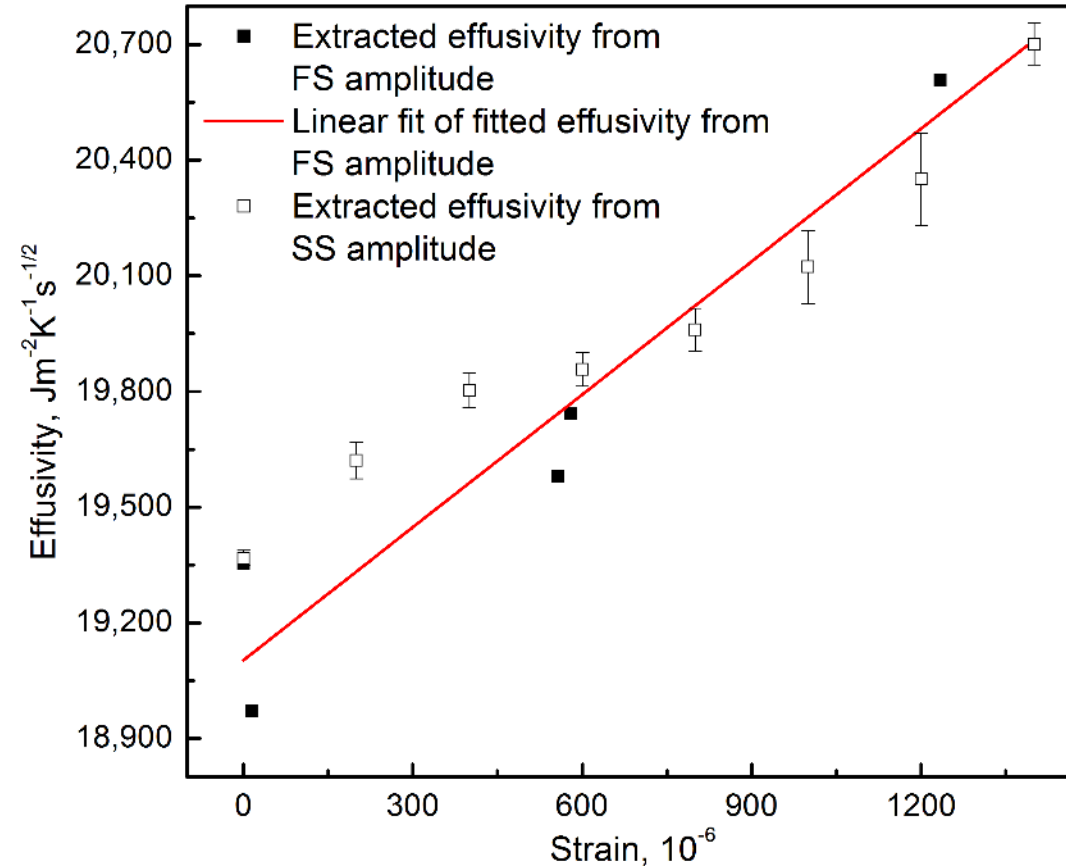
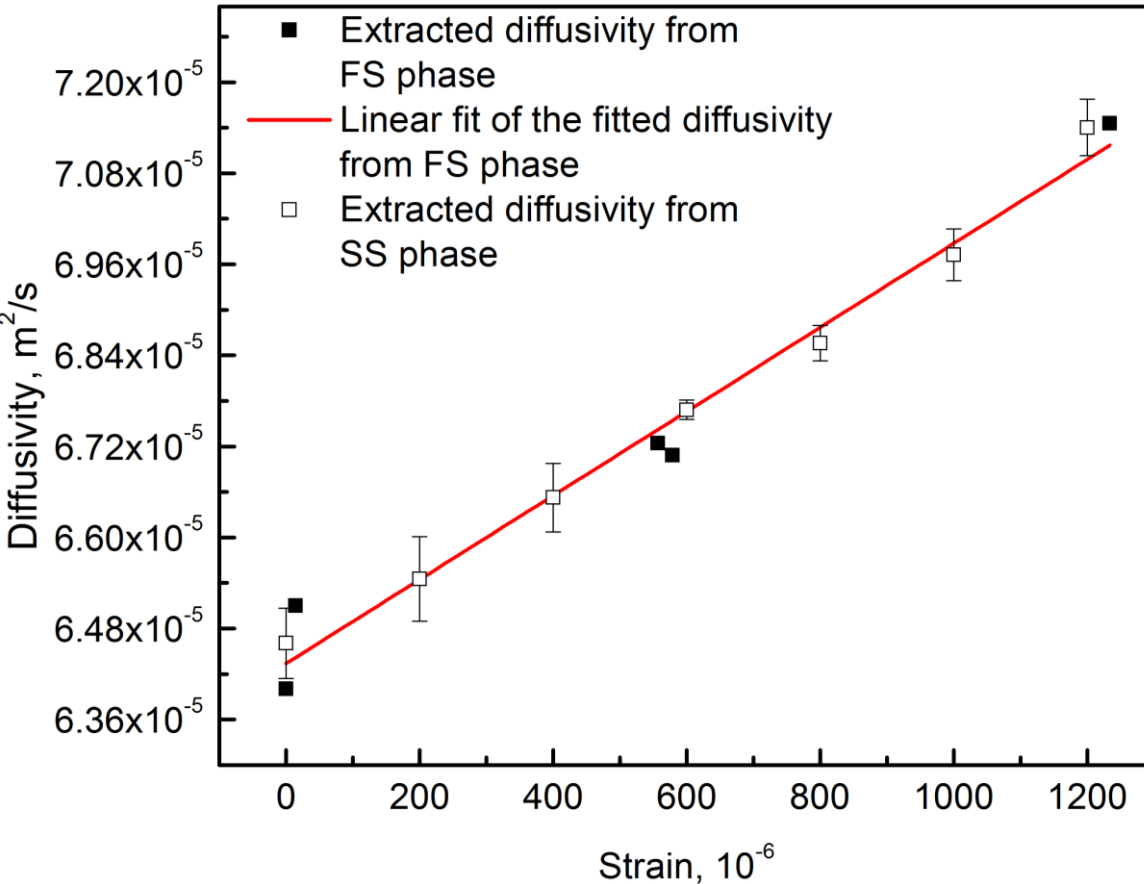
$$A(f) \sim \|Y(f)\| I_0(f) \left(\frac{1}{e_1 \sqrt{f}}\right) \frac{[(1 - e^{-2\gamma})^2 + 4e^{-2\gamma} \sin^2 \gamma]^{1/2}}{(1 - e^{-\gamma} \cos \gamma)^2 + e^{-2\gamma} \sin^2 \gamma}, \quad \Phi(f) = \arctan\left(\frac{-2e^{-\gamma} \sin \gamma}{1 - e^{-2\gamma}}\right) - \frac{\pi}{4}, \quad \gamma \equiv 2\sqrt{\pi f \kappa(\tau)}, \quad \kappa(\tau) \equiv L/\sqrt{\alpha(\tau)} \quad (4)$$

κ is the only parameter that affects the phase signal Eq. (4) while amplitude relies on both κ and e_1 . Fitting the phase curve can extract κ ; subsequent fitting the amplitude can yield e_1 .



Quantification Results

- Applying 1-D single layer thermal-wave model to the tensile test results, we can obtain diffusivity and effusivity as functions of strain within the elastic regime:
 - FS : Frequency scan
 - SS : Strain scan

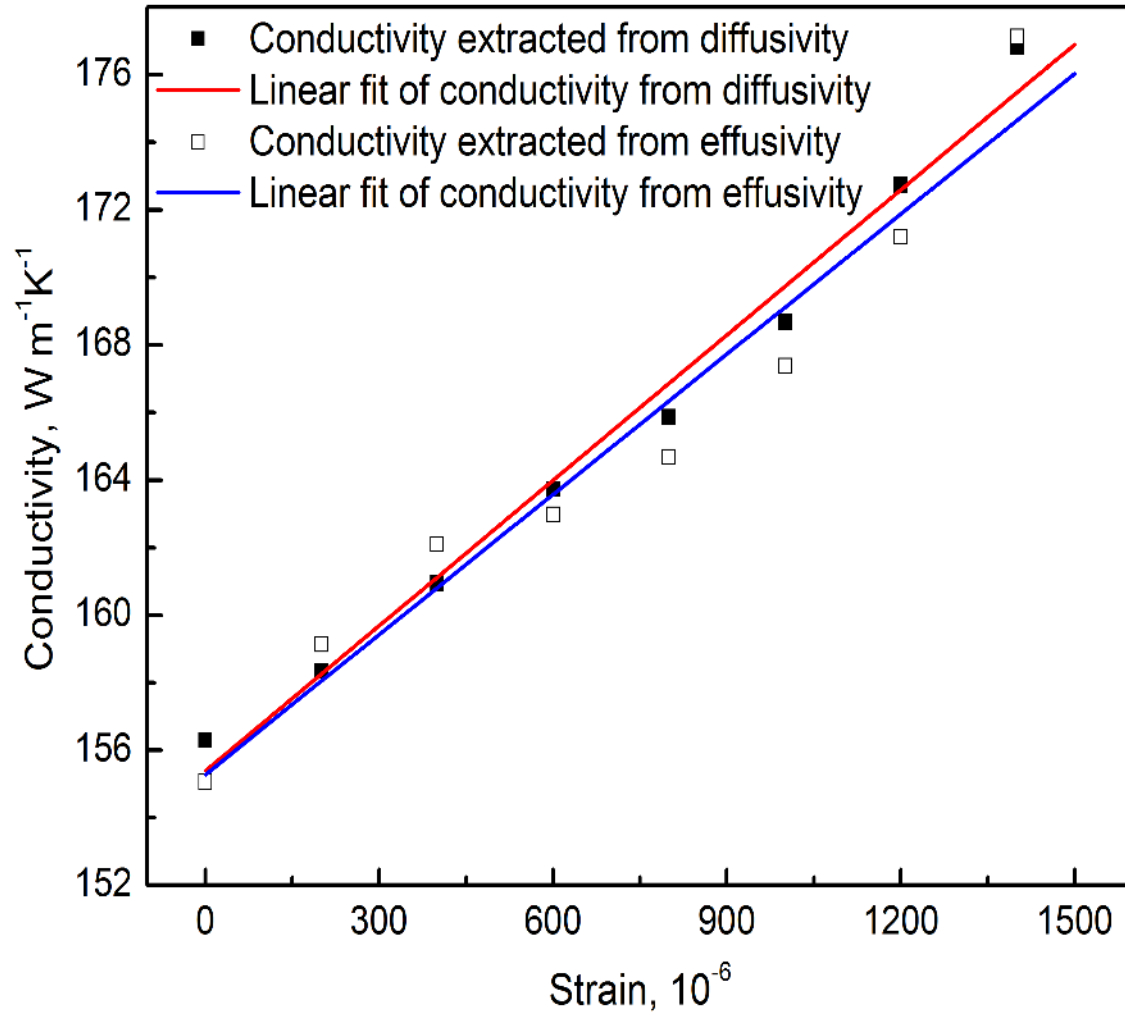


- Diffusivity increases with stress/strain: $\alpha(\varepsilon) = k / \rho C = 5.536 \times 10^{-3} \times \text{strain} + 6.434 \times 10^{-5} \text{ m}^2/\text{s}$
- Effusivity increases with stress/strain: $e_1(\varepsilon) = \sqrt{k \rho C} = 8.17 \times 10^5 \times \text{strain} + 19389.25 \text{ J}/(\text{m}^2 \text{Ks}^{1/2})$

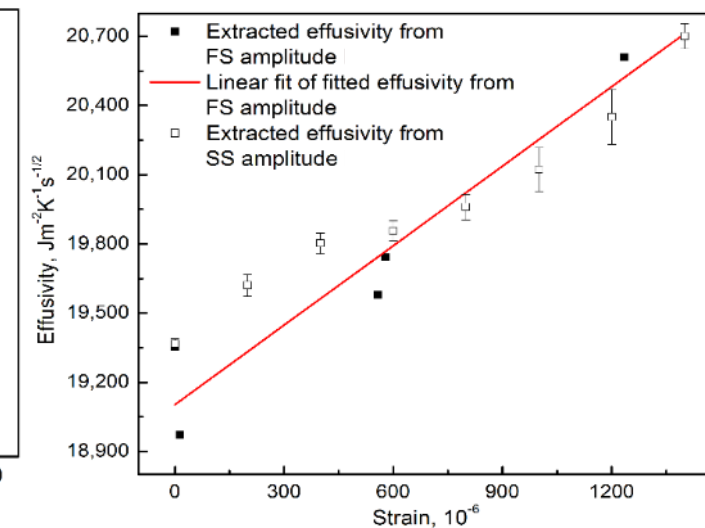
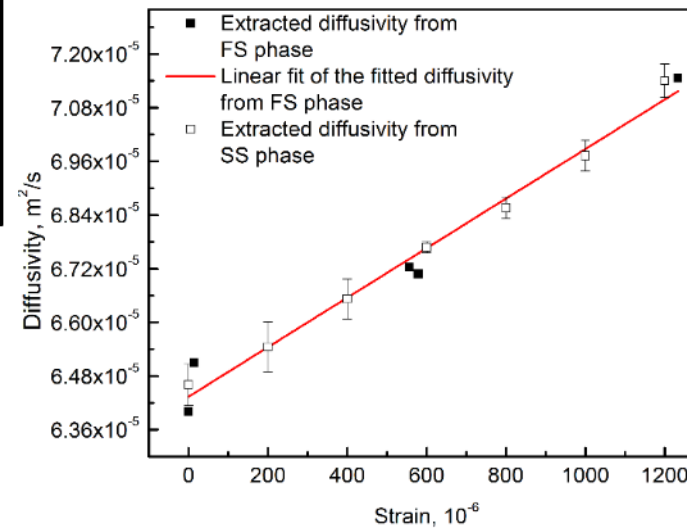
Results (cont'd)



- Comparison between effusivity- and diffusivity-derived thermal conductivity:

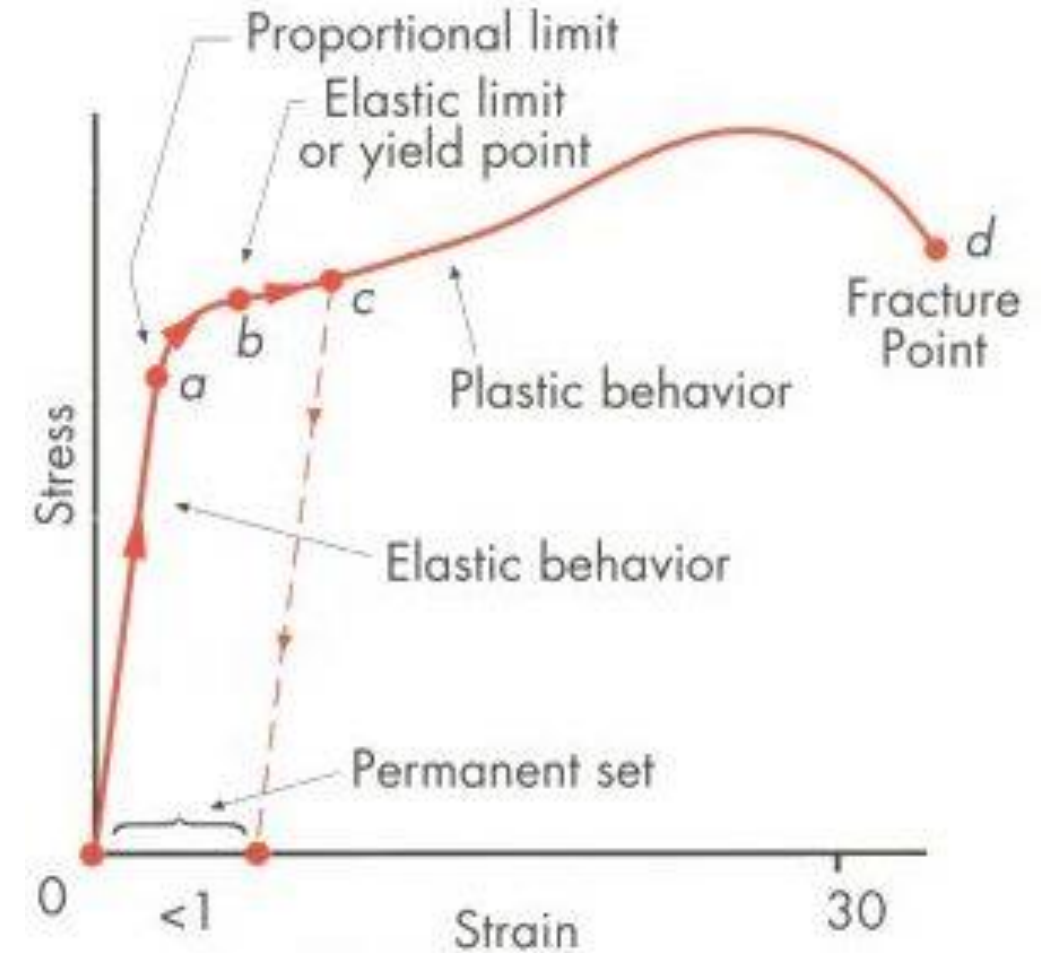
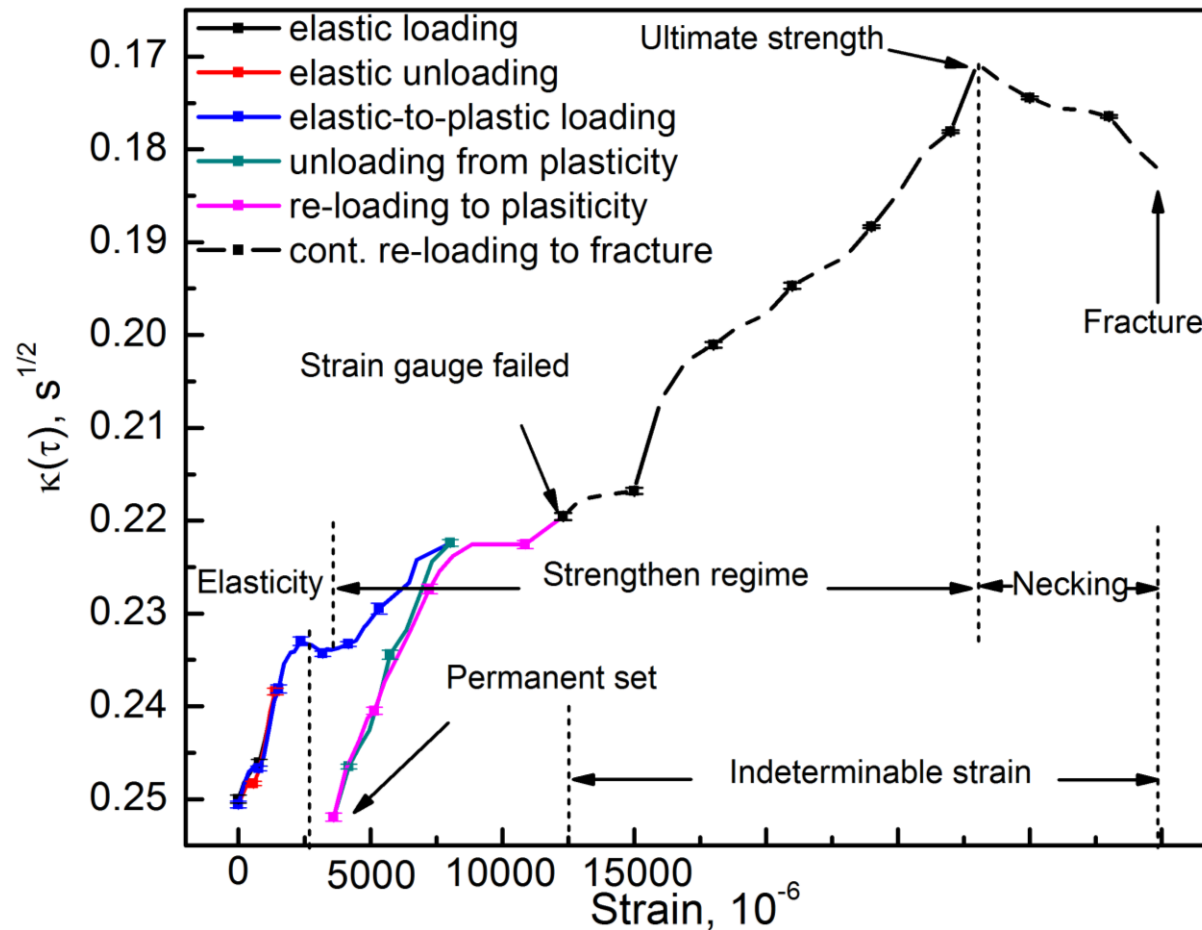


- Conductivity values obtained from two approaches show very good agreement.
- Conductivity shows linear dependence on strain within the elastic regime
- Thermal conductivity dependence on stress is the primary effect within the elastic regime



Analysis of Results

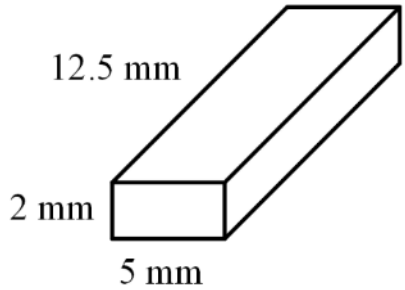
- Analogy: PTR phase-measured diffusivity-strain vs. stress-strain relation^[2]:



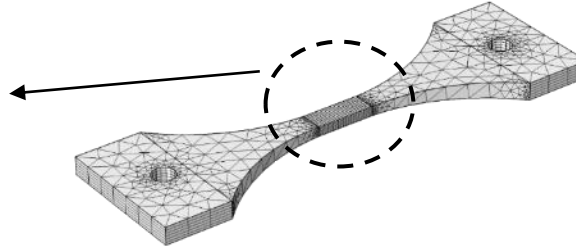
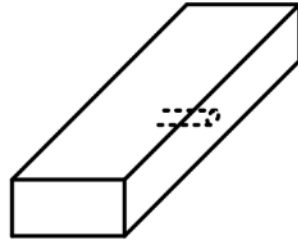
[2] Figure on the right from: <http://www.leonghuat.com/articles/civil%20engineering.htm>

Tests on Coated Samples

- The coated samples are:

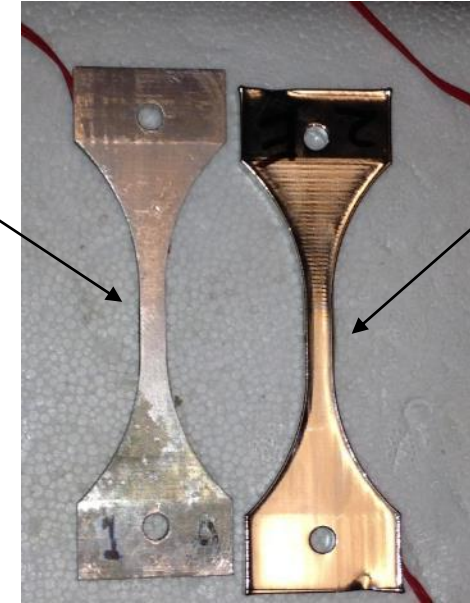


Sample 1: Substrate: intact dog-bone
Coating thickness: 0.005"



Sample 2: defective substrate with
coating (one hole at center, diameter:
1 mm, depth: ~1 mm)
Coating thickness: 0.005"

Uncoated sample

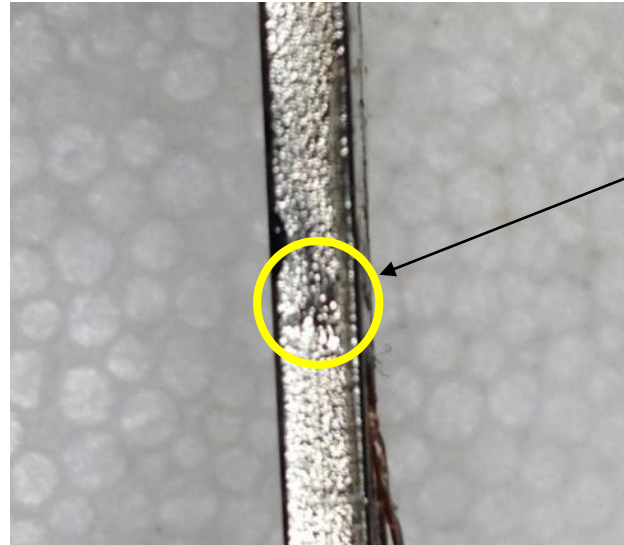


Coated sample

Intact
coated
sample



Defect: hole on
the substrate



- Experiments:
- Analysis:

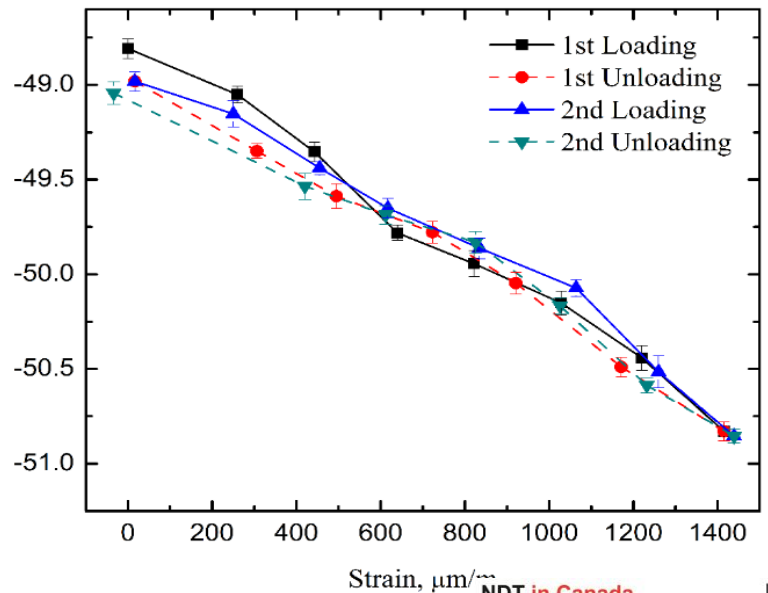
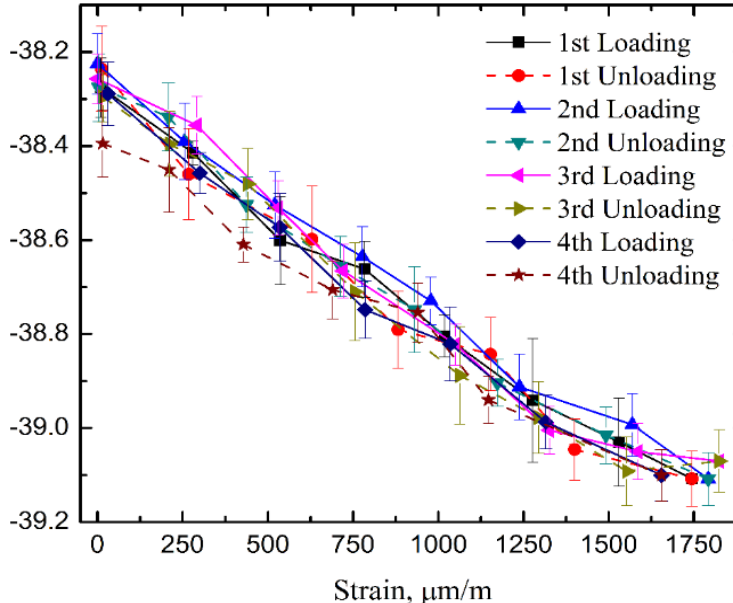
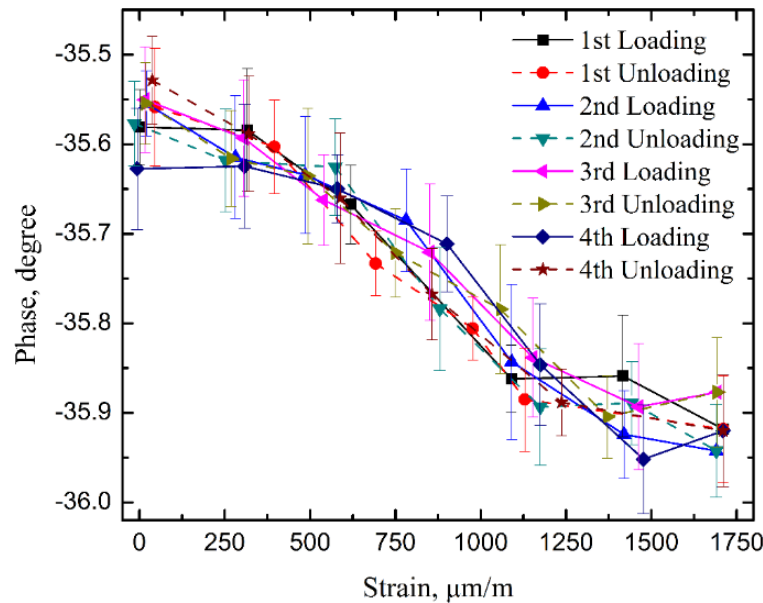
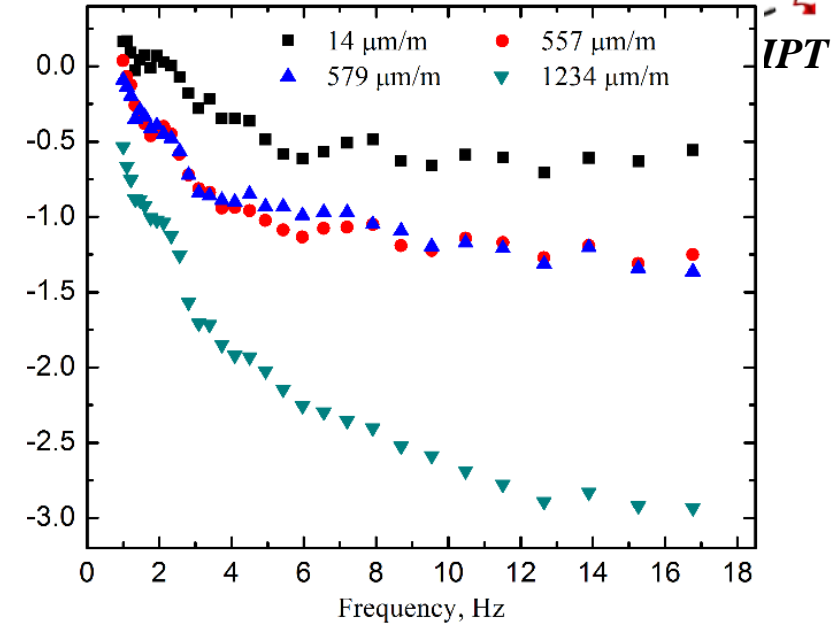
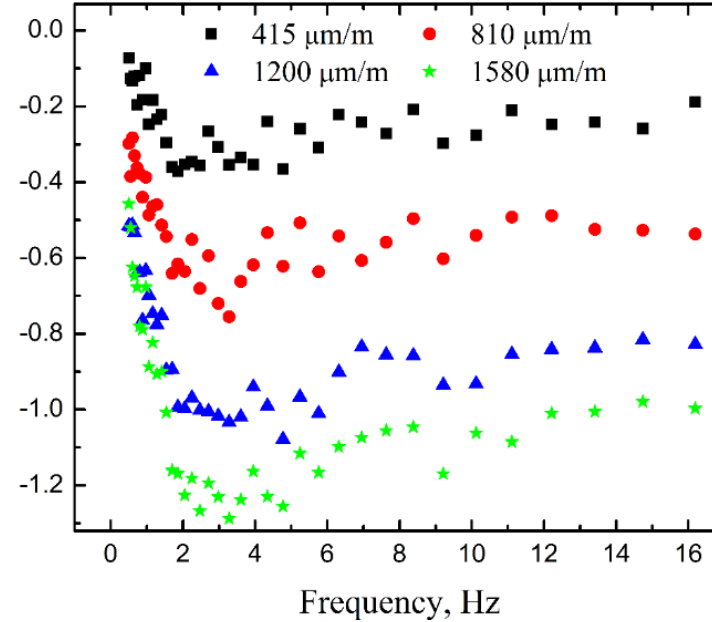
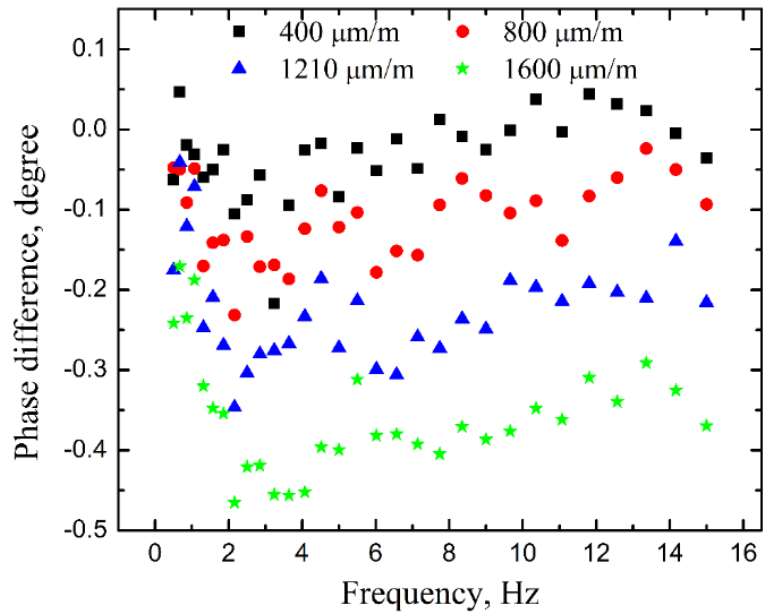
Frequency scan

Single layer model

Strain scan

Three-layer model

Coated Samples (cont'd)



Sample 1 (intact substrate)

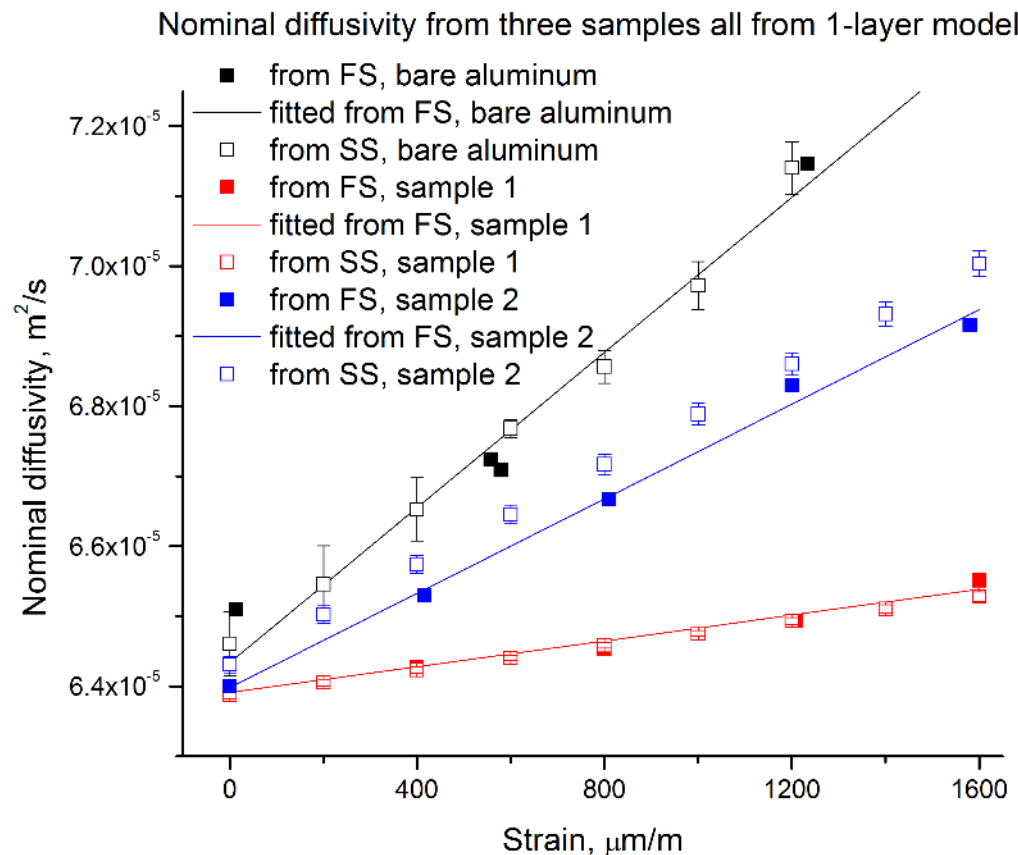
Sample 2 (defective substrate)

Bare aluminum

Coated Samples (cont'd)

- Quantification: single layer model (results)

Because the coated sample is not a single layer, the frequency range used for quantification should be low enough (0.5 Hz-5Hz). The results yield averaged overall thermal parameters for both coating and substrate.



- As the coated samples have different materials for substrate and coating, this single-layer model can only derive a nominal diffusivity which represents an approximate average diffusivity of the samples. The diffusivity of the aluminum substrate is chosen to be the nominal diffusivity for all three samples.
- Due to the existence of defects on the substrate of sample 2, best fits from FS and SS show larger differences than the other samples.

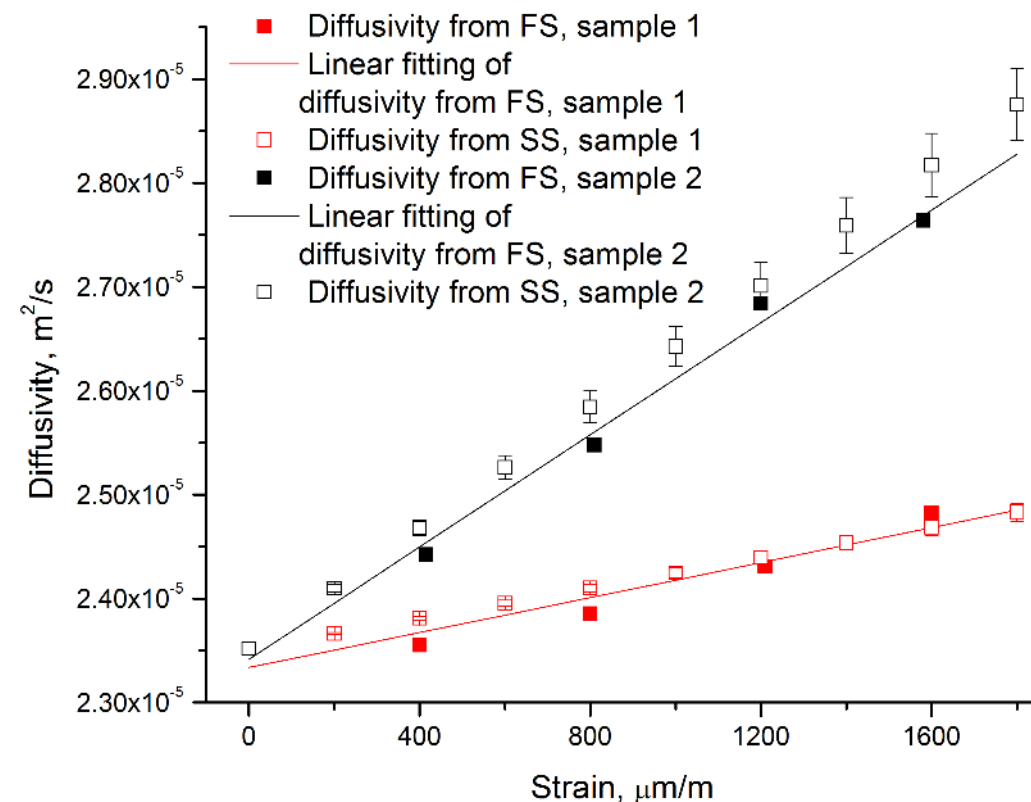
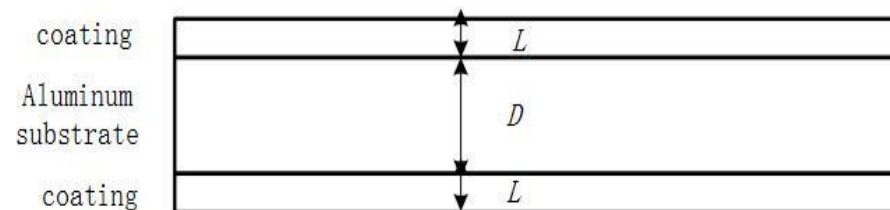
Coated Samples (cont'd)



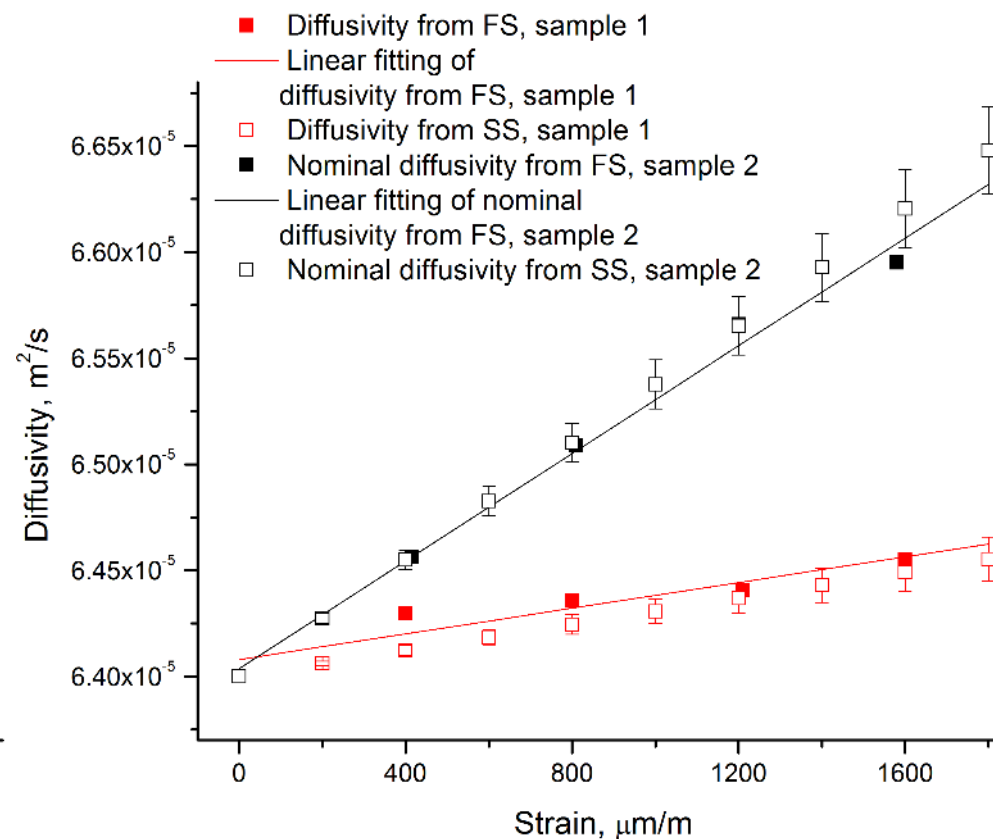
- Quantification: three-solid-layer model (results)

Frequency was scanned from 0.5 Hz to 15 Hz, and was fixed at 2.3 Hz for the intact sample and at 1.07 Hz for the defective substrate sample.

For the coating layer and substrate:



Coating diffusivity of the two coated samples



Substrate diffusivity of the two coated samples

● Compared with the single-layer results, the three layer model indicates diffusivity changes of both coating and substrate. For both, the changes are larger for the defective substrate.

Coated Samples (cont'd)

Discussion:

- Compared with the single-layer model, the three-layer model reveals more detailed information on the thermal conductivity strain dependencies of *both* coating and substrate materials
- The coated samples perform much better at the same strain than the bare aluminum sample: A comparison between coated and uncoated sample at fixed strain is shown below:

Strain at 1200 $\mu\text{m/m}$

Sample	Effective Diffusivity Change	NiCo coating Diffusivity Change	Aluminum Substrate Diffusivity Change
Bare Aluminum Alloy	11%	-	-
Sample1 (intact and coated)	1.6%	3.4%	0.55%
Sample 2 (Defective substrate coated)	6.1%	17%	2.3% (Effective)

It is hypothesized that for the defective aluminum substrate, the stretch is larger for both substrate and coating at the same strain, so the coating undergoes more deformation and thus larger thermal conductivity / diffusivity change. At the same level of strain, the defective substrate sample undergoes larger tensile loading because its “waist” is more “yielding” than the intact substrate. Thus, it elongates more and so does the coating.

Conclusions: Significance and Outlook



- A) PTMR analysis proved to be able to quantify mechanical property relations of aerospace-relevant metallic components under stress
- B) PTMR emerges as a non-contacting, non-destructive, quantitative “strain gauge” with a much expanded strain range compared to conventional contacting mechanical strain gauges. It works instantaneously and does not require long adhesive curing times (usually overnight).
- C) PTMR can quantify the mechanical performance of multilayer (coated) samples:
 - 1) It can assess the mechanical strength of NiCo coatings toward the protection of coated substrates through measurements of PTMR signals at fixed strain.
 - 2) It can assess the mechanical strength or improvement of defective substrates through coating and can quantify thermophysical changes of both coating and substrate upon mechanical stress application using stress scans and frequency scans.
 - 3) The elastic limits of solids can be identified and studied as functions of geometric shape, material and coating.
- D) PTMR can map the entire stress-strain cycle for uncoated and coated samples from the unstressed state through the elastic, plastic and fracture stages. *This is not possible for attached mechanical strain*

Future work



Having proven the feasibility of non-contact evaluation of mechanical property relations by the PTMR approach, further work for this methodology will include:

- Apply PTMR test with the application of mid-infrared camera to quantify the three conductivity components under multi-directional loading.
- Develop more complex, applicable 3-D quantitative thermal-wave theory and inverse algorithms to reconstruct the internal thermal conductivity tensor distribution from fitting the contours at various surfaces of the sample.
- Testing samples with known (or unknown) residual stresses

Acknowledgments



People. Discovery. Innovation.

**The Natural Sciences and Engineering
Research Council of Canada**



MINISTRY OF RESEARCH AND INNOVATION



Canada Research
Chairs

Chaires de recherche
du Canada

**The Canada Research Chairs
Program**

